

Temperature dependent tunneling spectroscopy in the heavy fermion CeRu_2Si_2 and in the antiferromagnet CeRh_2Si_2

A. Maldonado,¹ H. Suderow,^{1,*} S. Vieira,¹ D. Aoki,² and J. Flouquet²

¹*Laboratorio de Bajas Temperaturas,*

Departamento de Física de la Materia Condensada

Instituto de Ciencia de Materiales Nicolás Cabrera, Facultad de Ciencias

Universidad Autónoma de Madrid, 28049 Madrid, Spain

²*INAC, SPSMS, CEA Grenoble, 38054 Grenoble, France*

(Dated: June 11, 2022)

Abstract

CeRu_2Si_2 and CeRh_2Si_2 are two similar heavy fermion stoichiometric compounds located on the two sides of the magnetic quantum critical phase transition. CeRh_2Si_2 is an antiferromagnet below $T_N=36$ K with moderate electronic masses whereas CeRu_2Si_2 is a paramagnetic metal with particularly heavy electrons. Here we present tunneling spectroscopy measurements as a function of temperature (from 0.15 K to 45 K). The tunneling conductance at 0.15 K reveals V-shaped dips around the Fermi level in both compounds, which disappear in CeRu_2Si_2 above the coherence temperature, and above the Néel temperature in CeRh_2Si_2 . In the latter case, two different kinds of V-shaped tunneling conductance dips are found.

PACS numbers: 71.27.+a, 75.20.Hr, 68.37.Ef

*Corresponding author: hermann.suderow@uam.es

I. INTRODUCTION

Heavy fermion compounds show different ground states, e.g. paramagnetic (PM) Kondo lattice or antiferromagnetic (AF) Fermi liquid, with low critical temperatures that can be tuned by application of pressure or magnetic field[1–3]. Thus, they are key references for zero temperature quantum phase transitions. In particular, the so called magnetic quantum critical point (QCP) results when switching at zero temperature from AF order to PM phase at the critical pressure P_c . Parameters needed to describe this transition are the Kondo temperature (T_K), the intersite magnetic correlations which appear below T_{corr} , and the possible lift of the 4f angular momentum degeneracy by the crystal field splitting (Δ_{CF}). In addition, quasiparticles at the Fermi surface acquire its low temperature properties only when they are fully dressed below T_{coh} . During the last three decades, many studies sensing macroscopic and microscopic aspects of these compounds have provided new information about the behavior of a large number of them, especially in 4f (Ce and Yb) and in 5f (U) intermetallic compounds[1–3]. However, heavy fermion compounds are usually complex metals with many bands crossing the Fermi surface, often giving "spaghetti" like band structures (see [4, 5] for CeRu₂Si₂). Quantum oscillation experiments on the Fermi surface demonstrate that heavy fermions coexist with light itinerant carriers. The topology of the Fermi surface is generally well described by band structure calculations[5]. However, the derived calculated effective masses are often one or two orders of magnitude smaller than those experimentally found in the areas of the Fermi surface with heavy quasiparticles[4]. It is now believed that a large number of interesting effects appearing in these compounds are intimately related to the Fermi surface with mixed heavy and light electrons notably on Ce heavy fermion systems. Calculation methods have recently been improved and are able to deal in more detail with band structure experiments, and to help to understand atomic scale Scanning Tunneling Microscopy (STM)[6]. The latter opens new perspectives, providing direct information about electronic band structure and correlations. Successful STM measurements have been reported in PrOs₄Sb₁₂[7], PrFe₄P₁₂[8], YbRh₂Si₂[9], URu₂Si₂[10, 11] and in CeRhIn₅ and CeCoIn₅[12].

Our aim is to realize scanning tunneling spectroscopy in the two cerium tetragonal heavy fermion compounds CeRu₂Si₂ and CeRh₂Si₂ which are respectively in paramagnetic and antiferromagnetic ground state[3, 13]. In Fig. 1(a) we schematically show the situation of

both compounds in the phase diagram of heavy fermions in terms of the tuning parameter δ , which describes the competition between the local Kondo effect and the magnetic intersite interactions. In these compounds, the intersite magnetic correlations prevail over the single site Kondo effect. Furthermore, the crystal field splitting is strong enough to deal with Cerium doublet levels. The properties of both compounds are very well documented including de Haas Van Alphen measurements (see [4, 5] for CeRu₂Si₂ and [14] for CeRh₂Si₂).

CeRu₂Si₂ has a paramagnetic ground state and is close to a magnetic QCP. The electronic term in the specific heat, C/T , strongly increases when reducing temperature [3, 15, 16]. The Fermi liquid AT^2 law is found in the resistivity behavior only below $T_A = 1$ K [17]. Furthermore, the electronic Grüneisen parameter $\Omega_e(T)$ [18] has also a strong temperature variation at very low temperatures. At zero temperature, their respective extrapolations give $\gamma = (C/T)_{T \rightarrow 0} \sim 350$ mJmol⁻¹K⁻², $A \sim 1$ $\mu\Omega$ cmK⁻², $\Omega_e(T=0 \text{ K}) \sim +200$ and $T_{coh} \approx 9$ K. The QCP can be reached increasing the unit cell size by doping with La or Ge, implying that it is located at a slightly negative pressure of -0.3 GPa [19–22]. Effective masses range from 120 m_0 down to the bare electron mass m_0 [4].

Although the molar volume of CeRh₂Si₂ is smaller than that of CeRu₂Si₂ [23], the ground state of CeRh₂Si₂ is antiferromagnetic with a rather high Néel temperature $T_N \sim 36$ K [13, 24]. The sublattice magnetization is also rather large ($M_0 \sim 1.3\mu_B$) [25], generating a large molecular field. C/T decreases on cooling with a relatively small residual term $\gamma \sim 23$ mJmol⁻¹K⁻² [26, 27]. The Fermi liquid AT^2 term dominates the resistivity behavior already below 10 K, with $A \sim 1.4 \times 10^{-3} \mu\Omega$ cmK⁻² [28, 29]. The electronic Grüneisen parameter is negative with $\Omega_e \lesssim -20$ [26, 30]. Specific heat and thermal expansion have sharp maxima at T_N . Fermi surface experiments show effective masses ranging from 6 m_0 to 0.36 m_0 [5, 14, 31]. CeRh₂Si₂ is a compensated metal with large carrier number, which is also the case of CeRu₂Si₂ and YbRh₂Si₂ [2, 32], and with moderately heavy and light electrons.

The effective mass of the heavy carriers scales with the magnitude of γ and roughly with the inverse of T_{coh} . In the PM side of the QCP, the temperature T_A below which the Fermi liquid AT^2 law is obeyed is far lower than T_{coh} . In CeRh₂Si₂, antiferromagnetism with large T_N is the result of a strong interplay between local Kondo fluctuations and magnetic intersite interactions, clearly enhanced by switching from Ru to Rh ions. The effect of pressure is magnified by the proximity to an intermediate valence regime associated with the inefficiency of crystal field splitting (Δ_{CF}) when the Kondo temperature overpasses Δ_{CF} .

Antiferromagnetism disappears already below 1 GPa[14, 28–30].

The simple Doniach picture gives a Kondo temperature $T_K=25$ K for CeRu_2Si_2 and $T_K=50$ K for CeRh_2Si_2 [33, 34]. Specific heat and susceptibility measurements in CeRu_2Si_2 give a doublet crystal field ground state of Ising character located 200 K below the first excited level[15]. CeRh_2Si_2 also shows an Ising doublet crystal field ground state. Neutron scattering and susceptibility experiments suggest that the crystal field level is between 200 K and 600 K above the ground state[27, 33]. At first approximation, in the paramagnetic phase of Ce heavy fermion compounds, it is assumed that the Kondo temperature governs the high and intermediate temperature properties up to T_K and that the intersite interactions will play a role only below a temperature $T_{corr} < T_K$. However, in CeRu_2Si_2 microscopic inelastic neutron scattering experiments[19] as well as macroscopic measurements[17] such as magnetoresistivity, give $T_{corr} \sim 60$ K; i. e., higher than T_K . Thus the appearance of a resonance due to the interplay between the initial localized 4f electrons and the light itinerant (s, p, d) electrons is already renormalized by the intersite interactions.

Tunneling into a system with localized states such as Kondo ions or electrons with differing associated bands does not follow simple single particle tunneling theory[6, 9–11, 35, 36]. The tunneling conductance is not proportional to the density of states observed with macroscopic experiments, such as specific heat. Instead, it is the result of interference effects between the quasilocalized state, directly linked to the heavy carriers, and the light electron band, which couples to the tip’s light electron states[9–11]. A first approximation to account for multiparticle tunneling effects is to consider coherent tunneling through two interfering channels (Fig. 1(b)). The tunneling conductance can then be understood in terms of a Fano lineshape[37–41]. Depending on the dominance of each channel, from preferential tunneling into the quasilocalized states, to tunneling into the itinerant states, different shapes with different asymmetry, ranging from a peak into a dip, can be found in the tunneling conductance. As we show below, here we mainly observe a symmetric dip located at the Fermi level. Symmetric dips have been observed in tunneling experiments on single Ce adatoms[38], and they are interpreted as preferential tunneling into the itinerant electron channel, with a destructive interference to the quasilocalized ones, which reduces the conductance at the resonant level. Therefore, the tunneling conductance is given by an inverted Lorentzian function centered at zero bias voltage $g(V, T) = g_{off} + A \frac{(\frac{eV}{\Gamma})^2}{1+(\frac{eV}{\Gamma})^2}$, where Γ describes its width. This is equivalent to a modified Fano formula[37] with the asymmetry parameter

$q=0$ and the energy value where the resonance is centered $\epsilon_s=0$. We take $\Gamma(T=0\text{ K})$ to be of the order of the width of the heavy band, which inversely scales with the electronic effective mass m^* of the carriers in the heavy fermion compound.

II. EXPERIMENTAL DETAILS

The experimental set-up consists of a home-made STM in a Oxford Instruments MX400 dilution refrigerator with a positioning system which allows to change the scanning window of $2 \times 2 \mu\text{m}^2$ in-situ and without heating[42]. We use tips of Au which are prepared and cleaned in-situ as described in Ref. [43]. We obtain the tunneling conductance $g(V, T)$ by numerically derivating current vs bias voltage curves $I(V)$. $g(V, T) = dI/dV$ is normalized to the value obtained at a bias voltage well above 20mV. Single crystal samples of CeRu_2Si_2 and CeRh_2Si_2 were grown by Czochralski method as in previous work (see e.g.[13, 23]). We broke the samples along the basal plane of the tetragonal structure at ambient conditions immediately before mounting them on the STM and cooling down. Samples with a bright and optically flat surface were selected. In general, we found surfaces with rather irregular shapes (Fig.2) showing in some cases modulations at scales comparable to interatomic distances[44, 45]. Of course, some amount of surface contamination is unavoidable. In some particular cases, this could significantly influence tunneling features. The features discussed here are however reproducible, and the observed temperature ranges where they appear coincide with temperature ranges known from macroscopic measurements. Moreover, we have changed the scanning window using the macroscopic positioning system, and present results obtained over clean surfaces showing reproducible imaging.

III. RESULTS AND DISCUSSION

The tunneling conductance of CeRu_2Si_2 and CeRh_2Si_2 at 0.15 K reveals features consisting of a sharp V-shaped dip around zero bias voltage (Fig. 3). We find a different behavior in both materials. The V-shaped dip is wider for CeRh_2Si_2 than for CeRu_2Si_2 . In CeRh_2Si_2 we find two differing characteristic behaviors, with deep and shallow minima at zero bias, showing both roughly the same width. The dip disappears at 9.5 K for CeRu_2Si_2 , in good agreement with T_{coh} measured with thermal expansion. It remains up to a higher tempera-

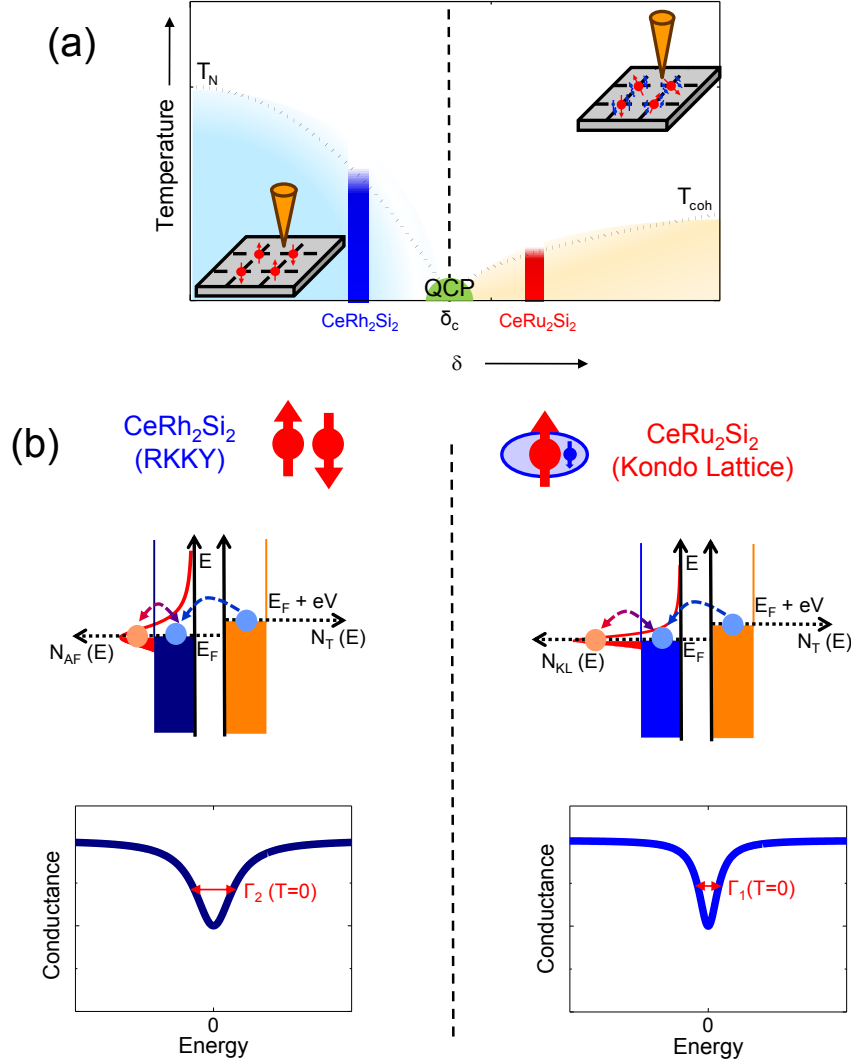


FIG. 1: (a) Sketch of the location of CeRu_2Si_2 and CeRh_2Si_2 within the T - δ phase diagram of heavy fermions, where δ is the tuning parameter which describes the competition between the local Kondo effect and the magnetic intersite interactions. Néel (T_N) and coherence (T_{coh}) temperatures are sketched as dashed black lines. The insets are cartoons of the experiment, with an Au tip tunneling into a Kondo lattice (CeRu_2Si_2) and into an antiferromagnet (CeRh_2Si_2). (b) Possible band diagrams for tunneling processes between an Au tip into a system with localized Kondo levels (left panel), and into a Kondo lattice (right panel) at zero temperature. The predominant tunneling channel is represented by blue dashed arrows, and the interaction with quasilocated states by reddish ones. The corresponding shape of the resulting tunneling conductance curves at $T=0$ K is represented in the lower panels.

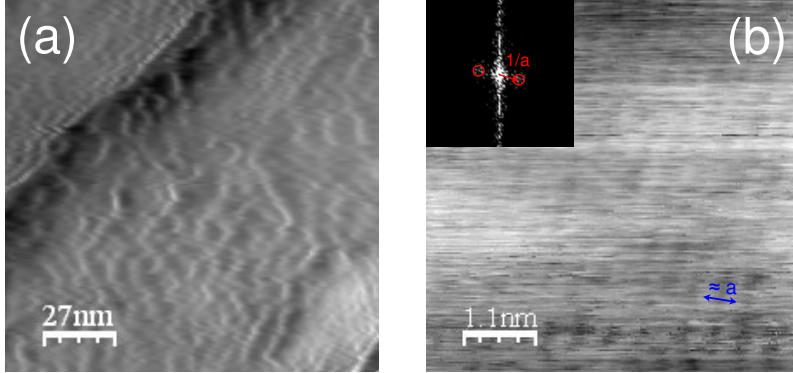


FIG. 2: Topography of CeRu_2Si_2 at 0.15 K taken at a conductance of $0.01 \mu\text{S}$ and a bias voltage of 50 mV in a scanning area of (a) $135 \text{ nm} \times 135 \text{ nm}$ (grey scale corresponds to height changes by 3 nm) and (b) $5 \text{ nm} \times 5 \text{ nm}$ (grey scale corresponds to height changes by 1 nm). Similar images are obtained in both compounds (CeRu_2Si_2 and CeRh_2Si_2). Inset shows the corresponding Fourier transform of the topography image, where the brightest Bragg peaks are highlighted by red circles. Their position in the reciprocal space, together with the period of the atomic scale features observed in the image, give a lattice parameter of about 0.4 nm.

ture, 45 K, for CeRh_2Si_2 (Fig.3). Fitting the conductance curves to the expression discussed above $g(V, T) = g_{off} + A \frac{(\frac{eV}{\Gamma})^2}{1 + (\frac{eV}{\Gamma})^2}$ we obtain the parameters discussed in Figs. 4 and 5. Γ is the resonance width. g_{off} and A are the zero bias voltage conductance and the amplitude of the dip, respectively. Both depend on the tip-sample wavefunction coupling and on the density of states of the sample at a given position. In Fig. 5 we show tunneling conductance curves for both compounds taken at different points of each sample surface, as well as the temperature dependence of the dip size g_{off} and width Γ .

The fits of the tunneling conductance curves at the lowest temperature (0.15 K) give a larger width Γ for the dips observed in CeRh_2Si_2 ($\Gamma_2(0.15 \text{ K}) \simeq 5.5 \text{ meV}$) than in CeRu_2Si_2 ($\Gamma_1(0.15 \text{ K}) \simeq 4 \text{ meV}$). Moreover, in CeRh_2Si_2 the two characteristic behaviors observed at 0.15 K, with a shallow and a deep V-shaped dip, show roughly the same width Γ_2 . The difference between both sets of curves is thus due to a different value of g_{off} .

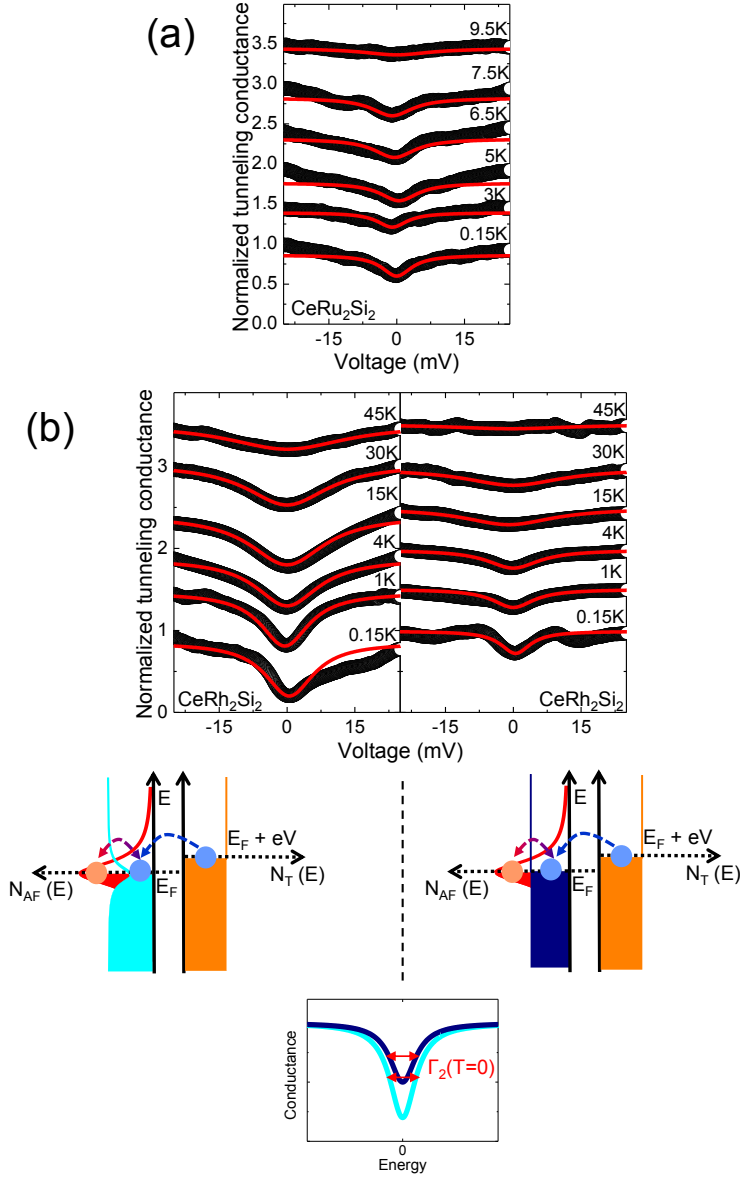


FIG. 3: The temperature evolution of the tunneling spectroscopy curves for (a) CeRu₂Si₂ and (b) CeRh₂Si₂ at an arbitrary position of their surfaces. Curves have been shifted by 0.5 for clarity. In the tunneling conductance curves of CeRh₂Si₂ at 0.15 K we find two characteristic behaviors, one with a deep V-shaped dip around zero bias voltage (left panel) and another with a shallow one (right panel). Red lines are fits to an inverted Lorentzian function as discussed in the text. The corresponding parameters are given in Fig. 4. In the lower panels of (b) band diagrams for tunneling processes between an Au tip and CeRh₂Si₂ at zero temperature are shown similarly as in Fig 1(b).

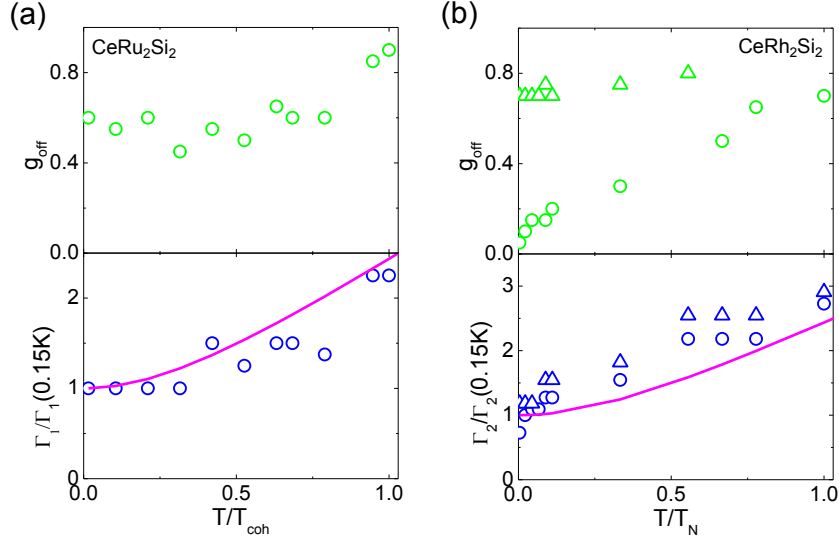


FIG. 4: Temperature evolution of the zero bias voltage conductance g_{off} and the width (Γ) of the dips revealed in the tunneling spectra normalized to its lowest temperature value for (a) CeRu_2Si_2 and (b) CeRh_2Si_2 (triangles for the shallow dips and circles for the strong dips observed in the tunneling conductance curves shown in Fig. 3). Temperatures have been normalized to the corresponding coherence ($T_{coh} \sim 9.5$ K) and Néel ($T_N \sim 45$ K) temperature for each compound. In the bottom panels we show (lines) the Fermi liquid fit, using the normalized equation indicated in the text.

In CeRu_2Si_2 , g_{off} changes with temperature only weakly, but Γ increases. In CeRh_2Si_2 we observe a temperature variation of g_{off} which is different depending on the shape of the curves. For the shallow dips, g_{off} do not vary significantly with temperature, as in CeRu_2Si_2 . However, for the deep V-shaped dips, g_{off} strongly increases. Γ increases with temperature similarly in both kinds of curves.

In both systems, despite the different values observed at low temperatures, Γ increases similarly with temperature. We can compare the thermal evolution of both Γ_1 and Γ_2 with the Fermi liquid prediction for temperature broadening of Γ normalized to its zero temperature value, $\Gamma(T=0)$, which can be written as $\Gamma/\Gamma(T=0) = \sqrt{\frac{1}{2}(\pi\frac{T}{T^*})^2 + 1}$ [46]. Here, we take T^* as the temperature for which the V-shaped dip disappears in CeRu_2Si_2 (T_{coh}) and the Néel (T_N) temperature for CeRh_2Si_2 . We observe that the thermal broadening of Γ

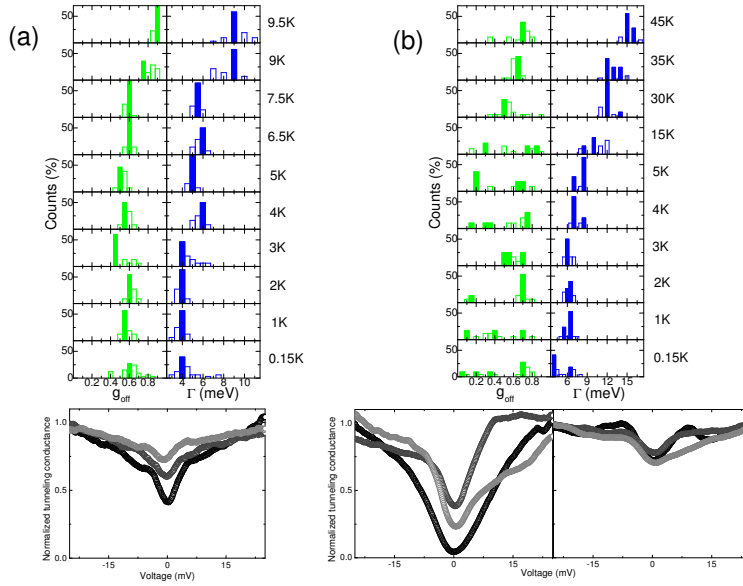


FIG. 5: Histograms for g_{off} and Γ obtained after fitting tens of tunneling conductance curves to the inverted Lorentzian function discussed in the text, which were taken at several different temperatures and at different positions of the surface of (a) CeRu_2Si_2 and (b) CeRh_2Si_2 . Lower panels show examples of the different tunneling spectra found at 0.15K over the surface of (a) CeRu_2Si_2 and (b) CeRh_2Si_2 .

for both compounds roughly follows the Fermi liquid prediction (bottom panel of Fig. 4). Therefore, the thermal smearing of the tunneling features is only determined by the characteristic energy scales for each compound, that are given by the corresponding values of Γ_1 and Γ_2 at 0.15K. Apart from the different energy scales obtained at the lowest temperatures, the temperature evolution of the tunneling features is roughly the same for CeRu_2Si_2 and CeRh_2Si_2 .

The weak temperature dependence of g_{off} observed in CeRu_2Si_2 is similar to the one observed in the thermal evolution of the tunneling spectra of URu_2Si_2 for temperatures above the hidden order transition[11]. In CeRh_2Si_2 we clearly find two different behaviors for g_{off} at different positions, which also evolve differently with temperature. This shows that long range magnetic order affects the tunneling signal. In CeRh_2Si_2 two antiferromagnetic sublattices appear at low temperature[25]. Possibly, additional gap opening or other features can give different tunneling conductance curves on specific surfaces. This can be re-inforced

by different behavior in the magnetic correlation lengths, as obtained in neutron scattering experiments. In CeRh_2Si_2 , it will rapidly reach atomic distances on cooling (after its divergence at T_N)[47]. In CeRu_2Si_2 , which is closer to the QCP, the magnetic correlation length increases smoothly on cooling being a few atomic distances at very low temperatures[48]. So that the Rh compound should be prone to show more local size surface dependent effects. It will be interesting to check the variations in the tunneling behavior when doping CeRu_2Si_2 with Rh[23], because it can unveil electronic features of magnetic interactions close to the quantum critical point.

IV. CONCLUSIONS

In conclusion, we have measured the features in the tunneling conductance curves of two Ce-based heavy fermion compounds (CeRu_2Si_2 and CeRh_2Si_2) as a function of temperature. We find V-shaped dips which signal heavy band formation in CeRu_2Si_2 and an antiferromagnetically ordered phase in CeRh_2Si_2 . The different temperature evolution of the observed zero bias V-shaped dip reflects the formation of different magnetic heavy-fermion ground states.

The Laboratorio de Bajas Temperaturas is associated to the ICMM of the CSIC. This work was supported by the Spanish MICINN and MEC (Consolider Ingenio Molecular Nanoscience CSD2007-00010 program, FIS2011-23488 and FPU grant), by the Comunidad de Madrid through program Nanobiomagnet and by ERC (NewHeavyFermion), and French ANR projects (CORMAT, SINUS, DELICE).

-
- [1] H. Lohneysen, A. Rosch, M. Votja, and P. Wolfle, *Rev. Mod. Phys.* **79**, 1015 (2007).
 - [2] P. Gegenwart, Q. Si, and F. Steglich, *Nat. Phys.* **4**, 186 (2008).
 - [3] J. Flouquet, *Progress in Low Temperature Physics* **15**, 139 (2005).
 - [4] M. Takashita, H. Aoki, T. Terashima, S. Uji, K. Maezawa, R. Settai, and Y. Onuki, *J. Phys. Soc. Japan* **65**, 515 (1996).
 - [5] M. Suzuki and H. Harima, *J. Phys. Soc. Japan* **79**, 024705 (2010).
 - [6] K. Haule and G. Kotliar, *Nature Physics* **5**, 796 (2009).

- [7] H. Suderow, S. Vieira, J. D. Strand, S. Bud'ko, and P. C. Canfield, *Phys. Rev. B* **69**, 060504(R) (2004).
- [8] H. Suderow, K. Behnia, I. Guillamon, V. Crespo, S. Vieira, D. Kikuchi, Y. Aoki, H. Sugawara, and H. Sato, *Phys. Rev. B* **77**, 153101 (2008).
- [9] S. Ernst, S. Kirchner, C. Krellner, C. Geibel, G. Zwicknagi, F. Steglich, and S. Wirth, *Nature* **474**, 362 (2011).
- [10] A. Schmidt, M. Hamidian, P. Wahl, F. Meier, A. Balatsky, J. Garrett, T. Williams, G. Luke, and J. C. Davis, *Nature* **465**, 570 (2010).
- [11] P. Aynajian, E. da Silva Neto, C. Parger, Y. Huang, A. Pasupathy, J. Mydosh, and A. Yazdani, *Proc. Nat'l. Acac. Sci USA* **107**, 10383 (2010).
- [12] P. Aynajian, E. H. da Silva Neto, A. Gyenis, R. E. Baumbach, J. D. Thompson, Z. Fisk, E. D. Bauer, and A. Yazdani, *Nature* **486**, 201 (2012).
- [13] W. Knafo, D. Aoki, D. Vignolles, B. Vignolle, Y. Klein, C. Jaudet, A. Villaume, C. Proust, and J. Flouquet, *Phys. Rev. B* **81**, 094403 (2010).
- [14] S. Araki, R. Settai, T. Kobayashi, H. Harima, and Y. Onuki, *Phys. Rev. B* **64**, 224417 (2001).
- [15] J. P. K. M. J. Besnus, P. Lehmann, and A. Meyer, *Solid State Commun.* **55**, 779 (1985).
- [16] R. A. Fisher, C. Marcenat, N. E. Phillips, P. Haen, F. Lapierre, P. Lejay, J. Flouquet, and J. Voiron, *J. Low Temp. Phys.* **84**, 49 (1991).
- [17] P. Haen, J. Flouquet, F. Lapierre, P. Lejay, and G. Remenyi, *J. Low Temp. Phys.* **67**, 391 (1987).
- [18] A. Lacerda, A. de Visser, P. Haen, P. Lejay, and J. Flouquet, *Phys. Rev. B* **40**, 8759 (1989).
- [19] W. Knafo, S. Raymond, P. Lejay, and J. Flouquet, *Nat. Phys.* **5**, 753 (2009).
- [20] S. Kambe, J. Flouquet, and T. E. Hargreaves, *J. Low Temp. Phys.* **108**, 383 (1997).
- [21] S. Quezel, P. Burlet, J. L. Jacoud, L. P. Regnault, J. Rossat-Mignod, C. Vettier, P. Lejay, and J. Flouquet, *J. Magn. Mater.* **76-77**, 403 (1988).
- [22] P. Haen, H. Bioud, and T. Fukuhara, *Physica B* **259-261**, 85 (1999).
- [23] D. Aoki, C. Paulsen, H. Kotegawa, F. Hardy, C. Meingast, P. Haen, M. Boukahil, W. Knafo, E. Ressouche, S. Raymond, et al., *J. Phys. Soc. Japan* **81**, 034711 (2012).
- [24] C. Godart, L. C. Gupta, and M. F. Ravet-Krill, *J. Less Common Metals* **94**, 187 (1983).
- [25] S. Kawarazaki, M. Sato, Y. Miyako, N. Chigusa, K. Watanabe, N. Metoki, Y. Koike, and M. Nishi, *Phys. Rev. B* **61**, 4167 (2000).

- [26] T. Graf, J. D. Thompson, M. F. Hundley, R. Movshovich, Z. Fisk, D. Mandrus, R. A. Fisher, and N. E. Phillips, *Phys. Rev. Lett.* **78**, 3769 (1997).
- [27] R. Settai, A. Misawa, S. Araki, M. Kosaki, K. Sugiyama, T. Takeuchi, K. Kindo, Y. Haga, E. Yamamoto, and Y. Onuki, *J. Phys. Soc. Japan* **66**, 2260 (1997).
- [28] S. Araki, M. Nakashima, R. Settai, T. C. Kobayashi, and Y. Onuki, *J. Phys. Condens. Matter* **14**, 377 (2002).
- [29] R. Boursier, A. Villaume, G. Lapertot, D. Aoki, G. Knebel, and J. Flouquet, *Physica B* **403**, 726 (2008).
- [30] A. Villaume, D. Aoki, Y. Haga, G. Knebel, R. Boursier, and J. Flouquet, *J. Phys. Condens. Matter* **20**, 015203 (2008).
- [31] M. Suzuki, Private communication (????).
- [32] G. Knebel, D. Aoki, J. P. Brison, and J. Flouquet, *J. Phys. Soc. Japan* **77**, 114704 (2008).
- [33] A. Severing, E. Holland-Moritz, and B. Frick, *Phys. Rev. B* **39**, 4164 (1989).
- [34] Y. Kawasaki, K. Ishida, Y. Kitaoka, and K. Asayama, *Phys. Rev. B* **58**, 8634 (1998).
- [35] M. Ternes, A. Heinrich, and W. Schneider, *J. Phys. Cond. Matt.* **21**, 053001 (2009).
- [36] M. Hamidian, A. Schmidt, I. Firmo, M. Allan, P. Bradley, J. Garrett, T. Williams, G. Luke, Y. Dubi, A. Balatsky, et al., *Proc. Nat'l. Acac. Sci USA* **108**, 18233 (2011).
- [37] U. Fano, *Phys. Rev.* **124**, 1866 (1961).
- [38] J. Li, W.-D. Schneider, R. Berndt, and B. Delley, *Phys. Rev. Lett.* **80**, 2893 (1998).
- [39] V. Madhavan, W. Chen, T. Jamneala, M. F. Crommie, and N. S. Wingreen, *Science* **280**, 567 (1998).
- [40] P. Wahl, L. Diekhoner, M. A. Schneider, L. Vitali, G. Wittich, and K. Kern, *Phys. Rev. Lett.* **93**, 176603 (2004).
- [41] J. Zhu, J. Julien, Y. Dubi, and A. Balatsky, *Phys. Rev. Lett.* **108**, 186401 (2012).
- [42] H. Suderow, I. Guillamon, and S. Vieira, *Rev. Sci. Inst.* **82**, 033711 (2011).
- [43] J. G. Rodrigo, H. Suderow, S. Vieira, E. Bascones, and F. Guinea, *J. Phys.: Condens. Matter* **16**, R1151 (2004).
- [44] S. Raymond, J. P. Rueff, S. M. Shapiro, P. Wochner, F. Sette, and P. Lejay, *Solid State Commun.* **118**, 473 (2001).
- [45] B. H. Grier, J. M. Lawrence, V. Murgai, and R. D. Parks, *Phys. Rev. B* **29**, 2664 (1984).
- [46] A. Schiller and S. Hershfield, *Phys. Rev. B* **61**, 9036 (2000).

- [47] J. Flouquet and H. Harima, *Kotai Butsuri* **2**, 47 (2012).
- [48] L. P. Regnault, J. L. Jacoud, J. L. Mignot, J. Rossat-Mignod, C. Vettier, P. Lejay, and J. Flouquet, *Physica B* **163**, 606 (1990).